

Article

A Generalized Fault Tolerant Control Based on Back EMF Feedforward Compensation: Derivation and Application on Induction Motors Drives

Mahdi Tousizadeh ^{1,*} , Amirmehdi Yazdani ^{2,*} , Hang Seng Che ¹ , Hai Wang ² , Amin Mahmoudi ³  and Nasrudin Abd Rahim ¹ 

¹ Higher Institution Centre of Excellence (HICoE), UM Power Energy Dedicated Advanced Centre (UMPEDAC), Level 4, Wisma R&D, University of Malaya, Jalan Pantai Baharu, Kuala Lumpur 59990, Malaysia

² College of Science, Health, Engineering and Education, Murdoch University, Perth 6150, Australia

³ College of Science and Engineering, Flinders University, Adelaide 5042, Australia

* Correspondence: toosizadeh@um.edu.my (M.T.); amirmehdi.yazdani@murdoch.edu.au (A.Y.)

Abstract: In this paper, a fault-tolerant three-phase induction drive based on field-oriented control is studied, and an analytical approach is proposed to elucidate the limitations of FOC in flux-torque regulation from the controller perspective. With an open-phase fault, the disturbance terms appear in the controller reference frame and degrade the controller performance when operating in a d - q plane with DC quantities. In addition, the hardware reconfiguration, which is essential to operate faulted three-phase drives, causes substantial change in the way the control parameters v_d , v_q are reflected onto the machine terminals. An accurate understanding of the feedforward term, by considering the open-phase fault and the hardware modifications, is provided to re-enable the FOC in presence of an open-phase fault. Furthermore, the concept of feedforward term derivation is generically extended to cover multiphase induction drives encountering an open-phase fault whereby no hardware reconfiguration is intended. The proposed method is explained based on a symmetrical six-phase induction and can be extended to drives with a higher number of phases. The effectiveness of the proposed derivation method, which is required to form a feedforward fault-tolerant controller, is verified and compared through the simulation and experiment, ensuring smooth operation in postfault mode.

Keywords: induction motors; fault-tolerant control; AC machines; back EMF; feedforward compensation



Citation: Tousizadeh, M.; Yazdani, A.; Che, H.S.; Wang, H.; Mahmoudi, A.; Rahim, N.A. A Generalized Fault Tolerant Control Based on Back EMF Feedforward Compensation: Derivation and Application on Induction Motors Drives. *Energies* **2023**, *16*, 51. <https://doi.org/10.3390/en16010051>

Academic Editors:

Daniel Morinigo-Sotelo,
Joan Pons-Llinares and
Rene Romero-Troncoso

Received: 21 November 2022

Revised: 12 December 2022

Accepted: 13 December 2022

Published: 21 December 2022



Copyright: © 2022 by the authors. Licensee MDPI, Basel, Switzerland. This article is an open access article distributed under the terms and conditions of the Creative Commons Attribution (CC BY) license (<https://creativecommons.org/licenses/by/4.0/>).

1. Introduction

Adjustable speed AC motor drives are, in general, susceptible to failure, especially in the power section where the stress is on the power switches and/or motor windings [1,2]. Since the failure might cause the whole drive to shut down, reliability is a key feature in applications in which a failure can cause safety issues. For example, fault-tolerant control of three-phase adjustable speed drives in automotive applications has recently attracted significant attention [3–6]. Thus, the need for an effective fault-tolerant method that can be embedded into the existing motor drives is practically favorable.

Since a three-phase machine with wye-connected stator winding will be effectively reduced to a “single-phase machine” under an OPF, topological reconfiguration is necessary for three-phase fault-tolerant drives to retain two degrees of freedom. In the literature, there are several feasible topologies used to reconfigure the three-phase AC drives [7–10]. Among these topologies, the majority of fault-tolerant three-phase drives utilize an additional inverter leg connected to the neutral point of the three-phase machine [11–14] as shown in Figure 1. Unless otherwise stated, this is considered the standard topology for fault-tolerant

three-phase drive hereafter [1,11,15]. This is to allow neutral current to return back to dc-link.

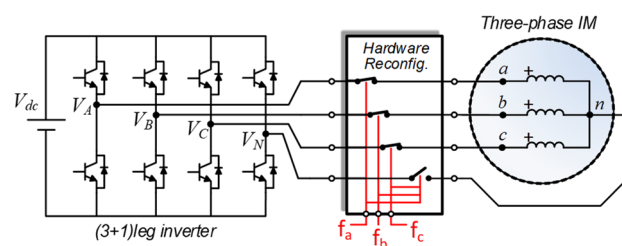


Figure 1. Fault-tolerant AC drive with (3 + 1) leg inverter and switches to emulate the open phase fault and reconfiguration. The signals f_a , f_b , and f_c are designed to emulate OPF on phase a, b, or c.

For multiphase (more than three phases) machines, however, the higher DOF allows the drive system to be inherently fault-tolerant towards OPF without the need for any hardware reconfiguration, as long as there are still three or more phases intact. Due to this higher fault tolerance, multiphase machines are often favored over their three-phase counterparts as fault-tolerant drives [16–19]. Regardless of the number of phases, OPFs always result in the loss of DOF in a drive and degrade the control performance if no mitigation measures are taken. In light of this, various fault-tolerant control techniques have been proposed in the past.

The mathematical model of the machine under OPF with a reduced order transformation matrix is attempted in [14,20–23]. It takes into account the reduced DOF and the unbalanced condition of the machine. While these methods were shown to be robust to machine parameter detuning, the re-derivation of machine models and reduced order transformation matrices are mathematically complex and unique for specific faults.

Alternatively, the original machine model and transformation can be maintained, and therefore, the effect of fault on the machine must be compensated by modifying the controller to handle double frequency in a d - q plane. For fault-tolerant three-phase drive, [13,24] demonstrated that the OPF gives rise to a negative sequence component and a negative sequence controller is needed to retain the current control performance in a positive sequence. For multiphase machines, analysis using the vector space decomposition method shows that OPFs create coupling between the torque-producing current components that are otherwise decoupled under healthy conditions [25,26]. The non-flux-and-torque-producing current components, also known as the x - y currents, are proportionally regulated to achieve fault tolerance [25,27]. These studies, for both three-phase and multiphase machines, utilize closed-loop feedback control methods where the unwanted current components are controlled using designated feedback current loop. However, as with any feedback control method, the dynamic performance during the transient will depend on the tuning of the controllers' parameters.

More recently, several research studies have highlighted the superiority of the feedforward compensation method being combined with a resonant controller for three-phase and six-phase drives [24,28]. The sensitivity of stator resistance to temperature, hence the inaccuracy of the feedforward term, is stated to be the main motivation for introducing an additional current controller to control the neutral current. However, this is not the only solution as the feedforward terms derived in the [11,12,29] are irrespective of stator resistance, which makes it robust against temperature variations. An accurate compensation term injected in a feedforward manner is shown to be effective for PMSM drives [11,12]. Similarly, for three-phase induction motors, feedforward compensation methods were introduced in [30,31] using the zero-sequence component.

Despite the documented research in the area of feedforward compensation methods for fault-tolerant induction motor drives, the following research questions still remain unaddressed:

1. How the concept of feedforward compensation can be realized from a control perspective in the context of FOC-driven AC drives?
2. How the feedforward compensation technique developed for three-phase machines can be extended for multiphase machines?

This paper is an extended version of the primary work presented in [29] to address the highlighted research questions. It expands the preliminary investigation on feedforward derivation and compensation techniques and the main contributions of this study are as follows:

1. An accurate feedforward compensation method based on FOC control and the open-phase fault is systematically derived that can be readily integrated into any three-phase AC drive with minimal modifications to the FOC controller. Furthermore, the stationary reference frame is used to apply the feedforward compensation as it simplifies the derivation complexities without any compromise in effectiveness.
2. The concept of feedforward term derivation is generically extended to a six-phase drive where the back EMF term is still the dominant part of the feedforward term but injected into a different plane to retain the control of the machine.

The organization of this paper is as follows. Section 2 discusses the fault tolerant control of a three-phase induction machine in both stationary and rotation reference frames, where the impacts of OPF on the mapping of the controlled variables to the machine variables are elucidated. In Section 3, the discussion is extended to a multiphase machine using a symmetrical six-phase machine as an example. Section 4 shows the experimental results, where the performances of the proposed feedforward compensation methods are verified using lab-scale three-phase and symmetrical six-phase induction machines. Finally, conclusions are given in Section 5.

2. Fault-Tolerant Control of Three-Phase Induction Machines

2.1. Mathematical Model of Three-Phase IM under RFOC

The dynamic model of the induction machine is usually given in the SRF d - q variables (and zero-sequence variable), which can be obtained from the phase variables using magnitude-invariant Clarke–Park transformation [32] as shown in (1):

$$T_3 = \frac{2}{3} \begin{bmatrix} \cos(\omega t) & \cos(\omega t - \delta) & \cos(\omega t + \delta) \\ -\sin(\omega t) & -\sin(\omega t - \delta) & -\sin(\omega t + \delta) \\ 0.5 & 0.5 & 0.5 \end{bmatrix} \quad (1)$$

where ω is the synchronous frequency of the machine and δ is the displacement factor of $2\pi/3$ a three-phase machine.

Based on the RFOC approach, the dynamic behavior of the induction machine can be expressed in terms of the stator voltage equations as follows:

$$\begin{bmatrix} v_{ds} \\ v_{qs} \\ v_{0s} \end{bmatrix} = \begin{bmatrix} R_s + \sigma L_s \rho & -\omega \sigma L_s & 0 \\ \omega \sigma L_s & R_s + \sigma L_s \rho & 0 \\ 0 & 0 & R_{s0} + L_0 \rho \end{bmatrix} \cdot \begin{bmatrix} i_{ds} \\ i_{qs} \\ i_{0s} \end{bmatrix} + \begin{bmatrix} \omega \frac{L_m}{L_r} \rho \\ \omega \frac{L_m}{L_r} \\ 0 \end{bmatrix} \cdot \psi_{dr} \quad (2)$$

where R_s , R_{s0} , L_m , L_r , L_0 , and σ are the stator resistance in the SRF plane, zero sequence resistance, magnetizing inductance, rotor self-inductance, zero sequence inductance and leakage factor of the induction machine, respectively. The leakage factor is defined to be $\sigma = 1 - (L_m^2 / L_s L_r)$. The synchronous angular speed of the machine in the electrical domain and rotor flux is denoted by ω and ψ_{dr} , respectively, where the symbol ρ represents the time-derivative of the variable. The rotor flux under RFOC is controlled directly by i_{ds} , known as flux current, to form a first-order system as

$$\psi_{dr} = \frac{L_m i_{ds}}{1 + \tau_r \rho} \quad (3)$$

with the rotor time constant τ_r being the ration of rotor self-inductance over the rotor resistance R_r .

2.2. Relation between Control Variables and Machine Variables

2.2.1. Healthy Operation

A typical three-phase induction motor drive system connected in a wye configuration and controlled under RFOC is depicted in Figure 2a. The main components of the drive are given in separate modules to elucidate how the control variables would be eventually mapped onto the machine under the healthy and postfault configuration.

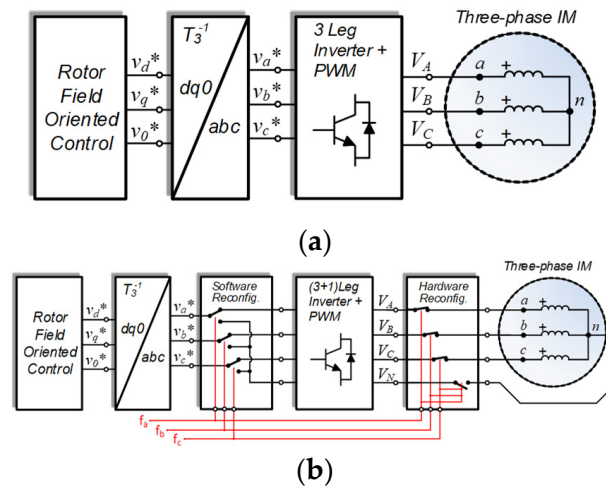


Figure 2. Three-phase induction motor drive with RFOC controller: (a) Typical topology for healthy operation, (b) Reconfigurable fault-tolerant topology with fault emulation signals f_n (n : a, b, c).

Starting with the machine on the rightmost part of Figure 2a, the phase windings are supplied through the leg voltage of the inverter V_A , V_B , and V_C . This configuration explicitly implies that the motor phase voltages v_{an} , v_{bn} , and v_{cn} are indirectly defined by the leg voltages of the inverter, as detailed in (4).

$$\begin{bmatrix} v_{an} \\ v_{bn} \\ v_{cn} \end{bmatrix} = \frac{2}{3} \begin{bmatrix} 1 & -0.5 & -0.5 \\ -0.5 & 1 & -0.5 \\ -0.5 & -0.5 & 1 \end{bmatrix} \begin{bmatrix} V_A \\ V_B \\ V_C \end{bmatrix} \tag{4}$$

The relation in (4) is valid for a balanced motor with all phases having equal impedance, which is the case for a healthy drive.

On the inverter block, the carrier-based PWM helps to form a voltage amplifier with a fixed gain of $K = V_{dc}/2$ that converts the modulating signals v_a^* , v_b^* , and v_c^* to leg voltages. The lumped transfer function of the inverter together with Sine PWM is given in a matrix in (5), assuming that inverter non-idealities are negligible, and no homopolar voltage is being injected.

$$\begin{bmatrix} V_A \\ V_B \\ V_C \end{bmatrix} = \begin{bmatrix} K & 0 & 0 \\ 0 & K & 0 \\ 0 & 0 & K \end{bmatrix} \begin{bmatrix} v_a^* \\ v_b^* \\ v_c^* \end{bmatrix} \tag{5}$$

One step before PWM, the control variables v_d^* , v_q^* , and v_0^* are basically transformed into modulating signals by applying the inverse Clarke–Park transformation given in (1).

$$\begin{bmatrix} v_a^* \\ v_b^* \\ v_c^* \end{bmatrix} = T_3^{-1} \begin{bmatrix} v_d^* \\ v_q^* \\ v_0^* \end{bmatrix} \tag{6}$$

By substituting (6) into (5) and (5) into (4), the relation between the control variable v_d^* and v_q^* and phase voltages received by the machine in matrix form is obtained to be as follow.

$$\begin{bmatrix} v_{an} \\ v_{bn} \\ v_{cn} \end{bmatrix} = K \begin{bmatrix} \cos(\omega t) & -\sin(\omega t) & 0 \\ \cos(\omega t - \delta) & -\sin(\omega t - \delta) & 0 \\ \cos(\omega t + \delta) & -\sin(\omega t + \delta) & 0 \end{bmatrix} \begin{bmatrix} v_d^* \\ v_q^* \\ v_0^* \end{bmatrix} \quad (7)$$

By applying (1) to both side of (7), the machine phase voltages would also be transformed into d - q -0 space, bringing everything to the same page (d - q -0), as stated in (8).

$$\begin{bmatrix} v_{ds} \\ v_{qs} \\ v_{0s} \end{bmatrix} = K \begin{bmatrix} 1 & 0 & 0 \\ 0 & 1 & 0 \\ 0 & 0 & 0 \end{bmatrix} \begin{bmatrix} v_d^* \\ v_q^* \\ v_0^* \end{bmatrix} \quad (8)$$

The terms v_{ds} , v_{qs} , and v_{0s} in (8) are in fact the transformed version of the stator phase voltages that correspond to the machine model in (2).

Accordingly, a couple of notable conclusions can be made from (8) which are valid for any wye connected three-phase AC drive, under healthy operation as:

C1: The voltage received by the motor in the synchronous frame (v_{ds} and v_{qs}) are directly proportional to the control variables (v_d^* and v_q^*) by a fixed gain of K . This unique property of healthy drive allows current controllers (such as PI controllers) in the SRF to control the flux and torque currents effectively;

C2: The zero-sequence voltage v_{0s} reached to the machine winding is not linked to v_0^* of the controller, making it decoupled from control variables (v_d^* and v_q^*).

2.2.2. Postfault Operation for Three-Phase Induction Motor Drive

Upon generation of fault flag f_n (n : a, b, c) in Figure 2b for the postfault topology, the following modifications are applied [11,13] to provide a path for neutral current to flow back to the dc-link:

m1: the fourth leg is clamped to the motor neutral point (according to hardware reconfiguration block in Figure 2b);

m2: the modulating signal of the faulted leg is switched over to the fourth leg (according to software reconfiguration block in Figure 2b).

To facilitate a quick transition to postfault operation for three-phase wye-connected drives, the fault must be detected in the first place, followed by hardware and software reconfigurations. However, fault detection is beyond the scope of this study, and the fault flag is created manually.

For the sake of simplicity, the fault and reconfigurations are simultaneously emulated by activating the corresponding fault signal, based on what has been shown in Figure 2b with red lines. Therefore, the relation stated in (8) needs to be re-examined, as the topology of the drive has been modified.

Assuming an OPF in phase a , i.e., by activation of f_a , the motor phase voltages in terms of leg voltage in postfault mode should be redefined as follow.

$$\begin{bmatrix} v_{an} \\ v_{bn} \\ v_{cn} \end{bmatrix} = \begin{bmatrix} 0 & 0 & 0 \\ -1 & 1 & 0 \\ -1 & 0 & 1 \end{bmatrix} \begin{bmatrix} V_N \\ V_B \\ V_C \end{bmatrix} + \begin{bmatrix} E_a \\ 0 \\ 0 \end{bmatrix} \quad (9)$$

where E_a is the back EMF voltage on the faulted phase and V_N is the leg voltage of the fourth leg. This induced voltage is basically due to the existence of rotating MMF in the machine. Since the motor phase a is disconnected from an inverter, the back EMF voltage E_a is no longer directly controllable by any inverter leg voltage, and therefore, is represented in a separate matrix in (9).

Once the modification $m2$ is executed, the active inverter leg voltages as a function of modulating signals would be the same as (5), with V_A being substituted with V_N .

$$\begin{bmatrix} V_N \\ V_B \\ V_C \end{bmatrix} = \begin{bmatrix} K & 0 & 0 \\ 0 & K & 0 \\ 0 & 0 & K \end{bmatrix} \begin{bmatrix} v_a^* \\ v_b^* \\ v_c^* \end{bmatrix} \quad (10)$$

Taking the same step as in (6) the relation between the control variables and phase voltage on the motor is obtained and stated in (11).

$$\begin{bmatrix} v_{an} \\ v_{bn} \\ v_{cn} \end{bmatrix} = \sqrt{3}K \begin{bmatrix} 0 & 0 & 0 \\ \cos(\theta_1) & -\sin(\theta_1) & 0 \\ \cos(\theta_2) & -\sin(\theta_2) & 0 \end{bmatrix} \begin{bmatrix} v_d^* \\ v_q^* \\ v_0^* \end{bmatrix} + \begin{bmatrix} E_a \\ 0 \\ 0 \end{bmatrix} \quad (11)$$

$$\theta_1 = \omega t - \delta - \frac{\pi}{6} \quad , \quad \theta_2 = \omega t + \delta + \frac{\pi}{6}$$

One step further, by applying the Clarke–Park transformation in (1) onto both sides of (11), the voltage relation in d - q -0 space after reconfiguration is found to be as follows:

$$\begin{bmatrix} v_{ds} \\ v_{qs} \\ v_{0s} \end{bmatrix} = K \begin{bmatrix} 1 & 0 & 0 \\ 0 & 1 & 0 \\ -\cos(\omega t) & \sin(\omega t) & 0 \end{bmatrix} \begin{bmatrix} v_d^* \\ v_q^* \\ v_0^* \end{bmatrix} + \frac{1}{3} \begin{bmatrix} 2E_a \cos(\omega t) \\ -2E_a \sin(\omega t) \\ E_a \end{bmatrix} \quad (12)$$

which is no longer the same as the healthy case stated in (8).

Equation (12) reveals that there exists a substantial double frequency AC disturbance on the machine winding in the d - q plane, whereas it is supposed to have all quantities in DC. The reconfigured drive, along with modifications $m1$ and $m2$, leads to the following observations:

Observation 1. *The OPF together with reconfiguration introduces double-frequency AC disturbance terms appearing on the d - q plane with the magnitude being proportional to the back EMF of the faulted phase.*

Observation 2. *The zero-sequence circuit of the motor is excited through the d - q voltages of the controller (v_d^* and v_q^*), and therefore, the machine voltages on the d - q -0 plane are now coupled under OPF.*

Observation 3. *The zero-sequence reference voltage on the controller side, v_0^* , still has no impact on either the zero sequence or the d - q components of the machine. Therefore, it can be ignored.*

As with the case of faulted PMSM discussed in [11], issue X1 is the main cause of control performance degradation in faulted three-phase induction drive even after converter reconfiguration. When PI controllers are used, the AC disturbance voltages disrupt the regulation of the d - q currents, due to the inability of PI controllers to completely suppress AC signals.

2.3. Feedforward Compensation for Fault-Tolerant Three-Phase Induction Motor Drive

From (12), it can be observed that by compensating the disturbance terms appearing on the right-hand side of the equation, one-to-one mapping of d - q voltages between the controller and the machine voltages will be restored. This can be done by calculating the terms and subtracting them from the control variables in the d - q plane in a feedforward manner, in a similar way as in [11].

$$v_{d_ff} = \frac{-2}{3K} E_a \cos(\omega t) \quad , \quad v_{q_ff} = \frac{2}{3K} E_a \sin(\omega t) \quad (13)$$

Alternatively, if the inverse Park transformation is applied to (12), the relation between controller and machine variables in the stationary reference frame (α - β -0) can be simplified as follows.

$$\begin{bmatrix} v_{\alpha s} \\ v_{\beta s} \\ v_{0s} \end{bmatrix} = K \begin{bmatrix} 1 & 0 & 0 \\ 0 & 1 & 0 \\ -1 & 0 & 0 \end{bmatrix} \begin{bmatrix} v_{\alpha}^* \\ v_{\beta}^* \\ v_0^* \end{bmatrix} + \frac{1}{3} \begin{bmatrix} 2E_a \\ 0 \\ E_a \end{bmatrix} \tag{14}$$

In this form, the disturbance terms need to be compensated in the α - β plane, as stated in (15).

$$v_{\alpha_ff} = \frac{-2}{3K} E_a \quad , \quad v_{\beta_ff} = 0 \tag{15}$$

Once the feedforward terms are added according to Figure 3, the AC disturbance terms in (12) or (14) would disappear such that;

- i. The C1 would hold true, and therefore, the RFOC would take over the control of the machine, just like the healthy drive, and
- ii. Unlike the healthy drive, there would be a non-zero voltage v_{0s} appearing on the zero-sequence circuit of the machine that is a function of control variables.

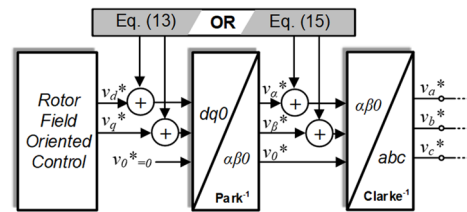


Figure 3. The two alternative planes for the injection of feedforward term(s) for three-phase IM drive.

After adding the feedforward term stated in (13) or (15), the zero-sequence voltage in postfault mode according to (12) or (14) would become

$$v_{0s} = -Kv_d^* \cos(\omega t) + Kv_q^* \sin(\omega t) + E_a = -Kv_{\alpha}^* + E_a \tag{16}$$

This should be in agreement with the machine equations given in (2) at steady state.

Since C1 is valid after feedforward injection (i.e., $Kv_d^* = v_{ds}$, and $Kv_q^* = v_{qs}$), the back EMF voltage E_a can be calculated by revisiting machine equations so that (16) would become

$$\begin{aligned} R_s 0i_{0s} + L_0 \rho i_{0s} &= -(R_s i_{ds} - \omega \sigma L_s i_{qs}) \cos(\omega t) + \\ & (R_s i_{qs} + \omega \sigma L_s i_{ds} + \omega L_m \psi_{dr} / L_r) \sin(\omega t) + E_a \end{aligned} \tag{17}$$

where the current relation in postfault mode is

$$i_{0s} = -i_d \cos(\omega t) + i_q \sin(\omega t) = -i_{\alpha} \tag{18}$$

Finally, by substituting (18) into (17) and neglecting the resistive terms, the steady state representation of back EMF voltage E_a is found to be as follows.

$$E_a = -\omega [((\sigma L_s - L_0) i_{ds} + \psi_{dr} L_m / L_r) \sin(\omega t) + (\sigma L_s - L_0) i_{qs} \cos(\omega t)] \tag{19}$$

Considering the feedforward terms obtained from (13) and (19), it is made clear that the back EMF voltage in (19), hence the feedforward term (13), is irrespective of stator resistance value. This important relation explicitly rules out the dependency of this feedforward compensation method on the machine temperature. Furthermore, a general analogy between the two types of machines, i.e., induction machine and PMSM, can be established. Due to the absence of saliency in the rotor structure of the IM, the σL_s in IM are found to be equivalent to L_d and L_q of the PMSM. Likewise, the equivalent term corresponding to the

permanent magnet flux (λ_{pm}) of PMSM is found to be $\psi_{dr}^* L_m / L_r$. This agreement suggests a further extension of the discussion to be detailed on the multiphase drives.

3. Fault-Tolerant Control of Six-Phase Induction Machines

3.1. Six-Phase Induction Machine Model under Rotor Field Oriented Control (RFOC)

For multiphase machines, analysis is usually performed based on the Vector Space Decomposition (VSD) model [33], where the machine variables can be decoupled into flux-and-torque producing α - β components, non-flux-and-torque producing x - y components and zero sequence 0_1 - 0_2 components. The concept of VSD transformation for multiphase machines with different phase numbers has been well-addressed in the literature on multiphase machines [26,34,35] and hence not dealt with further in this paper for brevity. To facilitate the subsequent discussion, a symmetrical six-phase induction machine with is used as a case study to represent a multiphase induction machine. The VSD model for a symmetrical six-phase induction machine controlled using RFOC is given in (20).

$$\begin{bmatrix} v_{ds} \\ v_{qs} \\ v_{xs} \\ v_{ys} \\ v_{01} \\ v_{02} \end{bmatrix} = \begin{bmatrix} R_s + \sigma L_s \rho & -\omega \sigma L_s & 0 & 0 & 0 & 0 \\ \omega \sigma L_s & R_s + \sigma L_s \rho & 0 & 0 & 0 & 0 \\ 0 & 0 & R_{sxy} + L_{xy} \rho & 0 & 0 & 0 \\ 0 & 0 & 0 & R_{sxy} + L_{xy} \rho & 0 & 0 \\ 0 & 0 & 0 & 0 & R_{s0} + L_0 \rho & 0 \\ 0 & 0 & 0 & 0 & 0 & R_{s0} + L_0 \rho \end{bmatrix} \cdot \begin{bmatrix} i_{ds} \\ i_{qs} \\ i_{xs} \\ i_{ys} \\ i_{01} \\ i_{02} \end{bmatrix} + \begin{bmatrix} \omega \frac{L_m}{L_r} \rho \\ \omega \frac{L_m}{L_r} \\ 0 \\ 0 \\ 0 \\ 0 \end{bmatrix} \cdot \psi_{dr} \quad (20)$$

By using rotational transformation, the α - β subspace can be rotated to form the synchronous d - q subspace, where the control of the machine in RFOC will be identical to that of a three-phase machine. Therefore, the rotor flux of a six-phase machine under RFOC is obtained in the same way as (3).

However, the x - y and 0_1 - 0_2 planes remain in a stationary reference frame as they are represented by a simple R - L circuit with no coupling to the rotor flux and do not contribute to flux-and-torque production.

3.2. Relation between Controller and Machine Variables

3.2.1. Healthy Operation

For a six-leg inverter driving a six-phase machine with star-connected stator winding and two isolated neutral, as shown in Figure 4, the motor phase voltages are a function of the inverter leg voltages as follows:

$$\begin{bmatrix} v_{a1n1} \\ v_{b1n1} \\ v_{c1n1} \\ v_{a2n2} \\ v_{b2n2} \\ v_{c2n2} \end{bmatrix} = \frac{1}{3} \begin{bmatrix} 2 & -1 & -1 & 0 & 0 & 0 \\ -1 & 2 & -1 & 0 & 0 & 0 \\ -1 & -1 & 2 & 0 & 0 & 0 \\ 0 & 0 & 0 & 2 & -1 & -1 \\ 0 & 0 & 0 & -1 & 2 & -1 \\ 0 & 0 & 0 & -1 & -1 & 2 \end{bmatrix} \begin{bmatrix} V_{A1} \\ V_{B1} \\ V_{C1} \\ V_{A2} \\ V_{B2} \\ V_{C2} \end{bmatrix} \quad (21)$$

where the leg voltages of (21) are determined through six modulating signals, as per Figure 4, in a similar condition as the three-phase case explained in (5).

$$[V_{A1} \ V_{B1} \ V_{C1} \ V_{A2} \ V_{B2} \ V_{C2}]^T = K[v_{a1}^* \ v_{b1}^* \ v_{c1}^* \ v_{a2}^* \ v_{b2}^* \ v_{c2}^*]^T \quad (22)$$

The modulating signals for the six-phase machine can be obtained by transforming the control variables using the extended inverse Clarke transformation (for symmetrical six-phase) as follow.

$$\begin{bmatrix} v_{a1}^* \\ v_{b1}^* \\ v_{c1}^* \\ v_{a2}^* \\ v_{b2}^* \\ v_{c2}^* \end{bmatrix} = \begin{bmatrix} 1 & 0 & 1 & 0 & 1.4142 & 0 \\ -0.5 & 0.866 & -0.5 & -0.866 & 1.4142 & 0 \\ -0.5 & -0.866 & -0.5 & 0.866 & 1.4142 & 0 \\ 0.5 & 0.866 & -0.5 & 0.866 & 0 & 1.4142 \\ -1 & 0 & 1 & 0 & 0 & 1.4142 \\ 0.5 & -0.866 & -0.5 & -0.866 & 0 & 1.4142 \end{bmatrix} \begin{bmatrix} v_{\alpha}^* \\ v_{\beta}^* \\ v_x^* \\ v_y^* \\ v_{01}^* \\ v_{02}^* \end{bmatrix} \quad (23)$$

Finally, by substituting (23) into (21)–(22) and applying extended Clarke transformation, the voltage relation in healthy operation arrives at (24) as follows.

$$\begin{bmatrix} v_{\alpha s} \\ v_{\beta s} \\ v_{x s} \\ v_{y s} \\ v_{01 s} \\ v_{02 s} \end{bmatrix} = K \begin{bmatrix} 1 & 0 & 0 & 0 & 0 & 0 \\ 0 & 1 & 0 & 0 & 0 & 0 \\ 0 & 0 & 1 & 0 & 0 & 0 \\ 0 & 0 & 0 & 1 & 0 & 0 \\ 0 & 0 & 0 & 0 & 0 & 0 \\ 0 & 0 & 0 & 0 & 0 & 0 \end{bmatrix} \begin{bmatrix} v_{\alpha}^* \\ v_{\beta}^* \\ v_x^* \\ v_y^* \\ v_{01}^* \\ v_{02}^* \end{bmatrix} \quad (24)$$

The relation between control variables and machine voltages for a symmetrical six-phase machine in (24) is harmonious to (8) whereby the α - β components, corresponding to a d - q plane, are directly controllable, as well as x - y components. Moreover, the v_{01s} and v_{02s} are still uncontrollable and isolated from one another since the machine is configured with two isolated neutrals. Till this point, the conclusions C1 and C2 are also valid for (24), however, the postfault relation is yet to be derived.

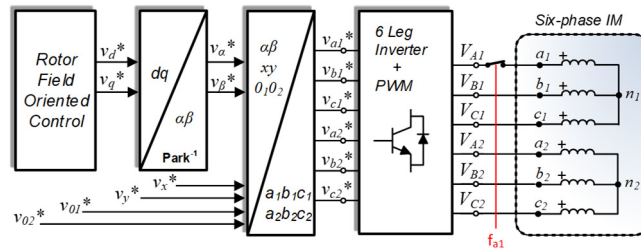


Figure 4. Six-phase induction motor drive (two isolated neutral) with RFOC and one reconfigurable OPF on phase a_1 . The signal f_{a1} is to emulate the OPF.

3.2.2. Postfault Operation

By introducing an OPF, emulated by a switch being triggered via f_{a1} in Figure 4, phase a_1 gets disconnected. As stated earlier, the six-phase drives do not require any hardware reconfiguration, as there exists a minimum DOF to control the machine in presence of an OPF. Nevertheless, the OPF alters the relation between the leg voltage and phase voltage of the machine, represented by the following matrix.

$$\begin{bmatrix} v_{a1n1} \\ v_{b1n1} \\ v_{c1n1} \\ v_{a2n2} \\ v_{b2n2} \\ v_{c2n2} \end{bmatrix} = \frac{1}{3} \begin{bmatrix} 0 & 0 & 0 & 0 & 0 & 0 \\ 0 & 1.5 & -1.5 & 0 & 0 & 0 \\ 0 & -1.5 & 1.5 & 0 & 0 & 0 \\ 0 & 0 & 0 & 2 & -1 & -1 \\ 0 & 0 & 0 & -1 & 2 & -1 \\ 0 & 0 & 0 & -1 & -1 & 2 \end{bmatrix} \begin{bmatrix} V_{A1} \\ V_{B1} \\ V_{C1} \\ V_{A2} \\ V_{B2} \\ V_{C2} \end{bmatrix} + \begin{bmatrix} E_{a1} \\ -0.5E_{a1} \\ -0.5E_{a1} \\ 0 \\ 0 \\ 0 \end{bmatrix} \quad (25)$$

With the connection between phase a_1 and leg V_{A1} being open-circuited in postfault, the remaining phases in the $a_1b_1c_1$ winding set will receive an AC term proportional to the back EMF of this faulted phase, E_{a1} , as given in Equation (25). By replacing (25) with (21)

and repeating the steps in section III-B-1, the voltage relation in postfault for a symmetrical six-phase machine would be given as (26).

$$\begin{bmatrix} v_{\alpha s} \\ v_{\beta s} \\ v_{xs} \\ v_{ys} \\ v_{01s} \\ v_{02s} \end{bmatrix} = K \begin{bmatrix} 0.5 & 0 & -0.5 & 0 & 0 & 0 \\ 0 & 1 & 0 & 0 & 0 & 0 \\ -0.5 & 0 & 0.5 & 0 & 0 & 0 \\ 0 & 0 & 0 & 1 & 0 & 0 \\ 0 & 0 & 0 & 0 & 0 & 0 \\ 0 & 0 & 0 & 0 & 0 & 0 \end{bmatrix} \begin{bmatrix} v_{\alpha}^* \\ v_{\beta}^* \\ v_x^* \\ v_y^* \\ v_{01}^* \\ v_{02}^* \end{bmatrix} + \begin{bmatrix} 0.5E_{a1} \\ 0 \\ 0.5E_{a1} \\ 0 \\ 0 \\ 0 \end{bmatrix} \quad (26)$$

Similar to (14), OPF in a six-phase machine introduces AC disturbance in the α -axis with the fundamental frequency. It is not hard to derive that this disturbance will appear as double frequency AC disturbances in the d - q frame ($0.5 E_{a1} \cos(\omega t)$ on the d -axis, $-0.5 E_{a1} \sin(\omega t)$ on the q -axis), analogous to what appeared in (12), which will cause the degradation of RFOC performance. Furthermore, (26) shows that there is a coupling between α - and x -axes, which is similar to the coupling between α - and 0 -axes for the case of the three-phase machine in (14).

3.3. Feedforward Compensation for Fault Tolerant Six-Phase Induction Motor Drive

To cancel the disturbance due to OPF in the α - β frame, the following steps are taken: Firstly, since the reference voltages in the α - and x -axes have opposite and equal coefficients in (26), the reference for the x -axis is derived directly from the α -axis and set to be exactly opposite as:

$$v_x^* = -v_{\alpha}^* \quad , \quad v_y^* = v_{\beta}^* \quad (27)$$

By substituting (27) into (26), the disturbance in the α -axis can be eliminated by adding a feedforward voltage to the v_{α}^* as follows.

$$v_{\alpha_ff} = \frac{-E_{a1}}{K} \quad , \quad v_{\beta_ff} = 0 \quad (28)$$

The implementation of (27) and (28) is illustrated in Figure 5.

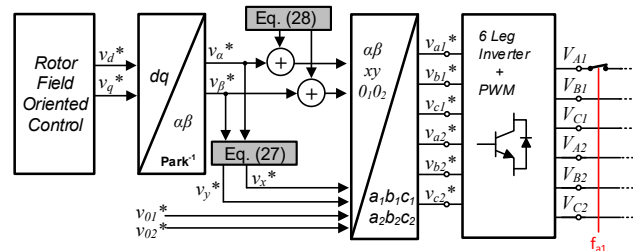


Figure 5. The injection of feedforward term(s) in symmetrical six-phase IM drive. The signal f_{a1} is to emulate the OPF.

As with a three-phase machine, the feedforward term requires the knowledge of the back EMF of the faulted phase. Through the application of (27) and (28), the voltage in the x -axis applied to the machine after injection of the feedforward term in (26) would be obtained as (29).

$$v_{xs} = -Kv_{\alpha}^* \cos(\omega t) + Kv_{\beta}^* \sin(\omega t) + E_{a1} = -Kv_{\alpha}^* + E_{a1} \quad (29)$$

Using a similar approach as in the three-phase case, the back EMF voltage E_{a1} needs to be derived. The voltage in the x -axis from the machine equation in (20) needs to be substituted into (29) to get E_{a1} as follows.

$$E_{a1} = -\omega [((\sigma L_s - L_{xy})i_{ds} + \psi_{dr}L_m/L_r) \sin(\omega t) + (\sigma L_s - L_{xy})i_{qs} \cos(\omega t)] \quad (30)$$

Equation (30) formulates the back EMF voltage of the lost phase on S6 in terms of the α - β parameters and operating. However, compared to three-phase IM, the zero sequence parameters are replaced with x - y , yet independent of stator resistance value. The effectiveness of the derived feedforward terms for symmetrical three- and six-phase machines is verified in the following section.

4. Results and Discussion

This section demonstrates the results of an experimental test conducted for the effectiveness and robustness validation of the proposed feedforward fault-tolerant control methodology. The experiment is performed using symmetrical three- and six-phase IM drives with the details given in Table 1. As shown in Figure 6, the motors are mechanically coupled with a passive load (1.8 kW PMSM feeding an adjustable resistor bank) and an incremental encoder (resolution 5000 pulse/rev) that is used to feedback on the speed. The phase current of the motor is measured through a six-channel current sensor (based on LEM current transducer). The motors are powered by a six-leg custom-made 12 kW inverter being supplied from a DC power supply (TDK Lambda GEN600-8.5). The RFOC control is implemented on the dSPACE DS1103 digital controller with a 5 kHz switching frequency.

Table 1. kW three-phase and 0.55 kW symmetrical six-phase induction motors.

	3-Phase IM	6-Phase IM
Power	1000 W	550 W
Phase Voltage	220 V	240 V
Phase Current	2.7 A	1.45 A
Speed	2800 RPM	1390 RPM
Frequency	50 Hz	50 Hz
Magnetizing Inductance Lm	490 mH	420 mH
Stator Leakage Inductance Lls	13 mH	6 mH
Stator Leakage Inductance Lxy	-	3.6 mH
Rotor Leakage Inductance Llr	13 mH	78 mH
Rotor Resistance	5.9 Ω	5.77 Ω
Flux Current, i_d	1.4 A	0.75 A



Figure 6. The experimental test rig for three-phase and six-phase induction motor drives under OPF.

The experiment is started by running the motors in healthy operation and after a while, a trigger signal is manually generated by the user to emulate the OPF using relay contacts. For the case of three-phase the modifications $m1$ and $m2$, as described in Figure 2b, are executed instantaneously together with OPF.

Figure 7 illustrates the transient section before and after OPF happening to the three-phase IM drive described in Figure 2b whereby both $m1$ and $m2$ are executed. Being in the postfault mode, the feedforward term shown in Figure 7b is calculated according to (15) and injected at $t = 0.2$ s. The irregularity of the phase currents before injection of the feedforward term, shown in Figure 7c, is highlighting the inability of the conventional PI current controller even if the DOF is more than 2. This is because the PI controller in the context of FOC is designed to handle DC quantities only. However, after $t = 0.2$ s the disturbances originating from OPF are canceled out by injecting the feedforward voltage. It eventually allows disturbance-free operation of the RFOC re-enabling the two PI current controllers to track the set point. From 0.2 s onward in Figure 7c, the waveform of phases b and c start to become equal in magnitude and 60 degrees apart to generate circular rotating MMF with two windings only.

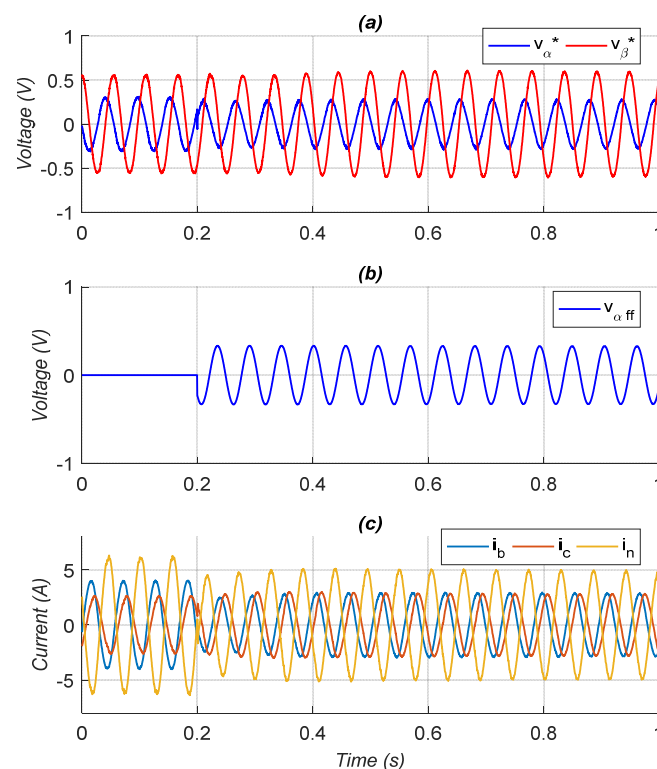


Figure 7. Postfault experimental result for the three-phase IM drive with feedforward injected at 0.2 s: (a) α - β voltage, (b) feedforward voltage, (c) phase and neutral current.

The experimental results show that feedforward injection successfully cancels out the disturbance, and hence, enables the current controller to regulate the circular trajectory of the α - β current, as illustrated in Figure 8a (highlighted by a circle). Unlike the healthy operation, the Figure 8b shows the elliptical shape of reference α - β voltage that has been supplied to the motor to have a circular trajectory of the α - β current in postfault mode. From the perspective of a rotating reference frame, the feedforward injection eventually blocks the severe double frequency oscillations in d - q current as well as mechanical speed, as depicted in Figure 9. Using the same approach as the three-phase IM, the symmetrical six-phase IM is driven in healthy mode first and one OPF is created on phase a_1 by means of relay contact. The waveform in Figure 10b shows the feedforward voltage that is obtained using (30) and has been injected according to (28) at $t = 0.2$ s. Due to OPF being phase a_1

and the neutral configuration of the drive, the phase current of b_1 and c_1 are forced to have equal and opposite magnitude, however, by implementing (27) together with feedforward injection from (28) at $t = 0.2$ s, the phase current of the set 2 is regulated to be unequal to restore circular current trajectory in the α - β plane, as illustrated in Figure 11a.

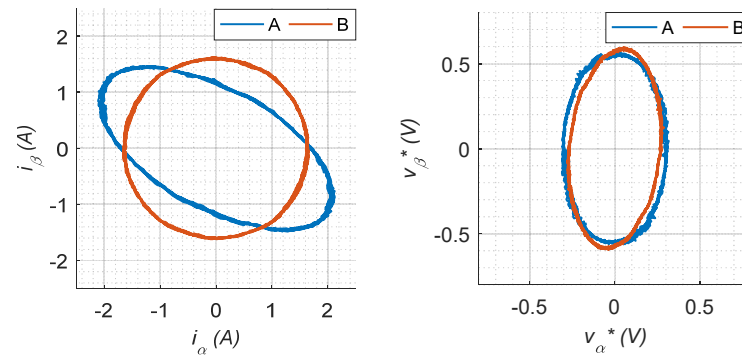


Figure 8. Trajectory of the current and voltage in α - β frame. A: before injection of feedforward, B: after injection of feedforward for three-phase IM.

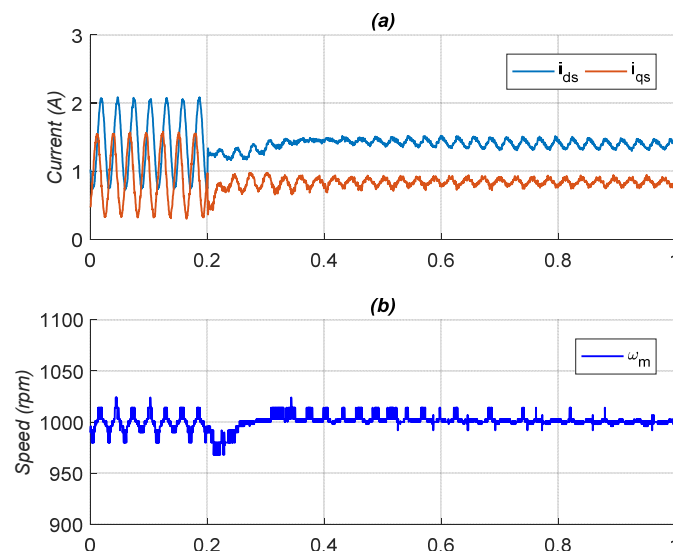


Figure 9. Postfault waveform of (a) the d - q current and (b) mechanical speed from the three-phase IM drive before and after feedforward injection at 0.2 s.

The suppression of double frequency AC oscillations in d - q current as well as mechanical speed in Figure 12 confirms the effectiveness of feedforward compensation on the S6 machine. It should be highlighted that feedforward compensation in the case of multiphase machines helps to remove AC disturbance terms caused by OPF. However, the speed oscillations of the symmetrical six-phase machine in Figure 12b due to one OPF are comparably lower than the three-phase counterpart in Figure 9b. This is one of the claimed advantages of multiphase drives in terms of fault tolerance which has been well-addressed in the literature. On top of tolerating the OPF fault in a feedforward manner, additional current control methods might be applied for multiphase drives to run the motor in maximum torque or minimum loss mode. However, this is not the case for the three-phase drives with an OPF.

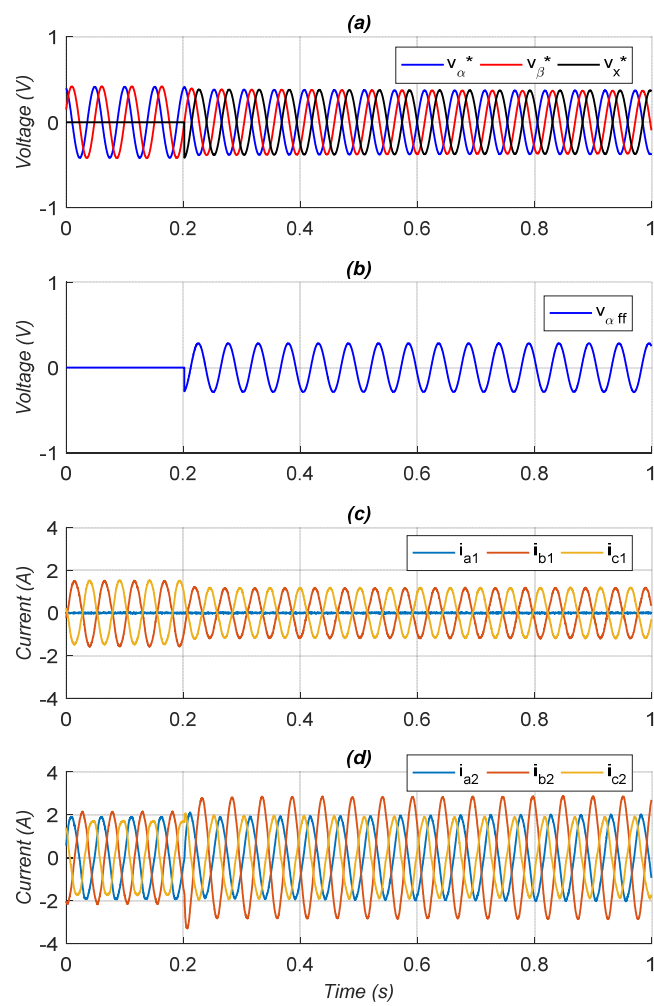


Figure 10. Postfault experimental result for the symmetrical six-phase IM drive with feedforward injected at 0.2 s: (a) α - β and x voltage, (b) feedforward voltage, (c) phase current of set1, (d) phase current of set 2.

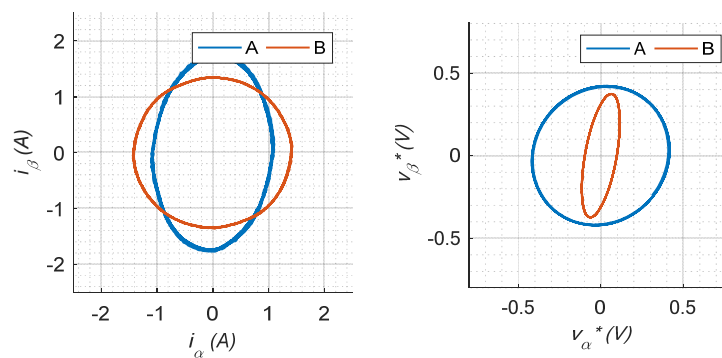


Figure 11. Trajectory of the current and voltage in α - β frame. A: before injection of feedforward, B: after injection of feedforward for symmetrical six-phase IM.

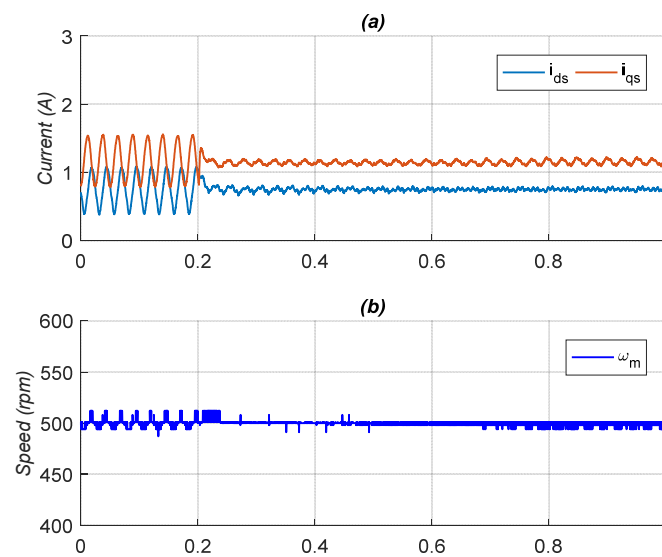


Figure 12. Postfault waveform of (a) the d - q current and (b) mechanical speed from the symmetrical six-phase IM drive before and after feedforward injection at 0.2 s.

5. Conclusions

In this paper, a generic analytical method is proposed to formulate the governing variables of FOC-driven AC drives under healthy and faulted conditions. This method considers the imposed and mandatory changes to the drive after OPF, if any, to specify how the control variables would be reflected in the machine terminals. The feedforward terms are subsequently derived based on a comparison of postfault relation to the healthy mode. The proposed method explicitly and generically formulates the feedforward terms to cancel out the undesired AC oscillatory terms expressed in both rotating and stationary reference frames. The experimental results of the symmetrical three- and six-phase machines verify the effectiveness of the proposed analytical method. Besides, the following salient findings can be noted:

- The feedforward compensation method, previously introduced for three-phase PMSM, has been re-derived in a generic way and applied to three-phase induction machines.
- The feedforward compensation on the stationary α - β reference frame is introduced instead of the d - q frame to make it immune to any error due to rotational transformations.
- The concept of feedforward compensation is further extended to multiphase induction machines, using a symmetrical six-induction machine as an example.
- It was shown that the feedforward term for a multiphase machine, like its three-phase counterpart, is a function of the back EMF voltage of the faulted phase, and independent of stator resistance value.

The future line of this study includes an investigation of the rapid fault detection schemes [36] incorporating the impact of small transient oscillation and DC offset [34] to be embedded into industrial drives, as well as commercial EVs [35,37].

Author Contributions: Conceptualization, M.T., A.Y. and H.S.C.; Methodology, M.T. and A.Y.; Software, M.T. and H.W.; Validation, M.T., A.Y. and H.S.C.; Formal analysis, M.T., H.S.C. and A.M.; Investigation, M.T.; Resources, H.W. and A.M.; Writing—original draft, M.T.; Writing—review and editing, M.T. and A.Y.; Supervision, H.S.C.; Project administration, M.T. and N.A.R.; Funding acquisition, H.S.C. and N.A.R. All authors have read and agreed to the published version of the manuscript.

Funding: This research was funded by Malaysian Ministry of Science and Technology, grant number FP090-2020.

Acknowledgments: Multiphase Machines Parameter Estimation Based on Drive Integrated Variable Extraction (DrIVE) Approach FP090-2020.

Conflicts of Interest: The authors declare no conflict of interest.

Nomenclature

AC	Alternating current
DC	Direct current
DOF	Degrees of freedom
DSRF	Double synchronous reference frame
FOC	Field-oriented control
FTC	Fault-tolerant control
MMF	Magnetomotive Force
OPF	Open-phase fault
PMSM	Permanent magnet synchronous machine
RFOC	Rotor field-oriented control
S6	Symmetrical six-phase
SRF	Synchronous reference frame

References

- Mirafzal, B. Survey of Fault-Tolerance Techniques for Three-Phase Voltage Source Inverters. *IEEE Trans. Ind. Electron.* **2014**, *61*, 5192–5202. [[CrossRef](#)]
- Behjati, H.; Davoudi, A. Reliability Analysis Framework for Structural Redundancy in Power Semiconductors. *IEEE Trans. Ind. Electron.* **2012**, *60*, 4376–4386. [[CrossRef](#)]
- Benbouzid, M.E.H.; Diallo, D.; Zeraoulia, M. Advanced Fault-Tolerant Control of Induction-Motor Drives for EV/HEV Traction Applications: From Conventional to Modern and Intelligent Control Techniques. *IEEE Trans. Veh. Technol.* **2007**, *56*, 519–528. [[CrossRef](#)]
- Naidu, M.; Gopalakrishnan, S.; Nehl, T.W. Fault-Tolerant Permanent Magnet Motor Drive Topologies for Automotive X-By-Wire Systems. *IEEE Trans. Ind. Appl.* **2010**, *46*, 841–848. [[CrossRef](#)]
- Wang, R.; Wang, J. Fault-Tolerant Control With Active Fault Diagnosis for Four-Wheel Independently Driven Electric Ground Vehicles. *IEEE Trans. Veh. Technol.* **2011**, *60*, 4276–4287. [[CrossRef](#)]
- Zhang, W.; Xu, D.; Enjeti, P.N.; Li, H.; Hawke, J.T.; Krishnamoorthy, H.S. Survey on Fault-Tolerant Techniques for Power Electronic Converters. *IEEE Trans. Power Electron.* **2014**, *29*, 6319–6331. [[CrossRef](#)]
- Tousizadeh, M.; Che, H.S.; Selvaraj, J.; Rahim, N.A.; Ooi, B.-T. Performance Comparison of Fault-Tolerant Three-Phase Induction Motor Drives Considering Current and Voltage Limits. *IEEE Trans. Ind. Electron.* **2018**, *66*, 2639–2648. [[CrossRef](#)]
- Wang, R.; Zhao, J.; Liu, Y. A Comprehensive Investigation of Four-Switch Three-Phase Voltage Source Inverter Based on Double Fourier Integral Analysis. *IEEE Trans. Power Electron.* **2011**, *26*, 2774–2787. [[CrossRef](#)]
- Van Der Broeck, H.W.; Van Wyk, J.D. A Comparative Investigation of a Three-Phase Induction Machine Drive with a Component Minimized Voltage-Fed Inverter under Different Control Options. *IEEE Trans. Ind. Appl.* **1984**, *20*, 309–320. [[CrossRef](#)]
- Liu, T.-H.; Fu, J.-R.; Lipo, T. A strategy for improving reliability of field oriented controlled induction motor drives. *IEEE Trans. Ind. Appl.* **1993**, *29*, 910–918. [[CrossRef](#)]
- Bolognani, S.; Zordan, M.; Zigliotto, M. Experimental fault-tolerant control of a PMSM drive. *IEEE Trans. Ind. Electron.* **2000**, *47*, 1134–1141. [[CrossRef](#)]
- Bianchi, N.; Bolognani, S.; Zigliotto, M.; Zordan, M. Innovative remedial strategies for inverter faults in IPM synchronous motor drives. *IEEE Trans. Energy Convers.* **2003**, *18*, 306–314. [[CrossRef](#)]
- Correa, M.B.D.R.; Jacobina, C.B.; da Silva, E.C.; Lima, A.N. An induction motor drive system with improved fault tolerance. *IEEE Trans. Ind. Appl.* **2001**, *37*, 873–879. [[CrossRef](#)]
- Gaeta, A.; Scelba, G.; Consoli, A. Modeling and Control of Three-Phase PMSMs Under Open-Phase Fault. *IEEE Trans. Ind. Appl.* **2013**, *49*, 74–83. [[CrossRef](#)]
- Tousizadeh, M.; Che, H.S.; Abdel-Khalik, A.S.; Munim, W.; Selvaraj, J.; Rahim, N.A. Effects of flux derating methods on torque production of fault-tolerant polyphase induction drives. *IET Electr. Power Appl.* **2021**, *15*, 616–628. [[CrossRef](#)]
- Lu, H.; Li, J.; Qu, R.; Ye, D.; Lu, Y. Fault-Tolerant Predictive Control of Six-Phase PMSM Drives Based on Pulsewidth Modulation. *IEEE Trans. Ind. Electron.* **2019**, *66*, 4992–5003. [[CrossRef](#)]
- Peng, Z.; Zheng, Z.; Li, Y.; Liu, Z. Machine Drives Based on Virtual Winding Method. In Proceedings of the 2017 IEEE Transportation Electrification Conference and Expo (ITEC), Chicago, IL, USA, 22–24 June 2017; pp. 252–256.
- Sun, J.; Liu, Z.; Zheng, Z.; Li, Y. An Online Global Fault-Tolerant Control Strategy for Symmetrical Multiphase Machines With Minimum Losses in Full Torque Production Range. *IEEE Trans. Power Electron.* **2020**, *35*, 2819–2830. [[CrossRef](#)]
- Moraes, T.D.S.; Nguyen, N.K.; Semail, E.; Meinguet, F.; Guerin, M. Dual-Multiphase Motor Drives for Fault-Tolerant Applications: Power Electronic Structures and Control Strategies. *IEEE Trans. Power Electron.* **2017**, *33*, 572–580. [[CrossRef](#)]
- Zhao, Y.; Lipo, T. Modeling and control of a multi-phase induction machine with structural unbalance: Part I. Machine modeling and multi-dimensional current regulation. *IEEE Trans. Energy Convers.* **1996**, *11*, 570–577. [[CrossRef](#)]

21. Ryu, H.-M.; Kim, J.-W.; Sul, S.-K. Synchronous Frame Current Control of Multi-Phase Synchronous Motor —Part II Asymmetric Fault Condition due to Open Phases. *IEEE Trans. Ind. Appl.* **2006**, *42*, 1062–1070.
22. Zhou, H.; Yang, G.; Wang, J. Modeling, Analysis, and Control for the Rectifier of Hybrid HVdc Systems for DFIG-Based Wind Farms. *IEEE Trans. Energy Convers.* **2011**, *26*, 340–353. [[CrossRef](#)]
23. Zhou, X.; Sun, J.; Li, H.; Song, X. High Performance Three-Phase PMSM Open-Phase Fault-Tolerant Method Based on Reference Frame Transformation. *IEEE Trans. Ind. Electron.* **2018**, *66*, 7571–7580. [[CrossRef](#)]
24. Xu, J.; Guo, S.; Guo, H.; Tian, X. Fault-Tolerant Current Control of Six-Phase Permanent Magnet Motor With Multifrequency Quasi-Proportional-Resonant Control and Feedforward Compensation for Aerospace Drives. *IEEE Trans. Power Electron.* **2023**, *38*, 283–293. [[CrossRef](#)]
25. Tani, A.; Mengoni, M.; Zarri, L.; Serra, G.; Casadei, D. Control of Multiphase Induction Motors With an Odd Number of Phases Under Open-Circuit Phase Faults. *IEEE Trans. Power Electron.* **2011**, *27*, 565–577. [[CrossRef](#)]
26. Che, H.S.; Duran, M.J.; Levi, E.; Jones, M.; Hew, W.-P.; Rahim, N.A. Postfault Operation of an Asymmetrical Six-Phase Induction Machine With Single and Two Isolated Neutral Points. *IEEE Trans. Power Electron.* **2013**, *29*, 5406–5416. [[CrossRef](#)]
27. Munim, W.N.W.A.; Duran, M.J.; Che, H.S.; Bermudez, M.; Gonzalez-Prieto, I.; Rahim, N.A. A Unified Analysis of the Fault Tolerance Capability in Six-Phase Induction Motor Drives. *IEEE Trans. Power Electron.* **2016**, *32*, 7824–7836. [[CrossRef](#)]
28. Guo, Y.; Wu, L.; Huang, X.; Fang, Y.; Liu, J. Adaptive Torque Ripple Suppression Methods of Three-Phase PMSM During Single-Phase Open-Circuit Fault-Tolerant Operation. *IEEE Trans. Ind. Appl.* **2020**, *56*, 4955–4965. [[CrossRef](#)]
29. Tousizadeh, M.; Yazdani, A.M.; Che, H.S.; Rahim, N.A. Feedforward Fault-Tolerant Control for Three-Phase Induction Motor Drives with Single Open Circuit Fault. In Proceedings of the 2019 International Conference on Power and Energy Systems (ICPES), Perth, WA, Australia, 10–12 December 2019; pp. 1–6. [[CrossRef](#)]
30. Jasim, O.; Sumner, M.; Gerada, C.; Arellano-Padilla, J. Development of a new fault-tolerant induction motor control strategy using an enhanced equivalent circuit model. *IET Electr. Power Appl.* **2011**, *5*, 618–627. [[CrossRef](#)]
31. Tousizadeh, M.; Che, H.S.; Selvaraj, J.; Abd Rahim, N.; Ooi, B.T. Fault-Tolerant Field Oriented Control of Three-Phase Induction Motor based on Unified Feed-forward Method. *IEEE Trans. Power Electron.* **2019**, *34*, 7172–7183. [[CrossRef](#)]
32. Krause, P.C.; Wasynczuk, O.; Sudhoff, S.D. *Analysis of Electric Machinery and Drive Systems*, 3rd ed.; IEEE Press: Piscataway, NJ, USA, 2002.
33. Levi, E. Multiphase Electric Machines for Variable-Speed Applications. *IEEE Trans. Ind. Electron.* **2008**, *55*, 1893–1909. [[CrossRef](#)]
34. Mule, G.J.A.; Munim, W.N.W.A.; Tousizadeh, M.; Abidin, A.F. Post-fault tolerant of symmetrical six-phase induction machine under open circuit fault with single and two isolated neutral points using graphical user interface. *AIP Conf. Proc.* **2019**, *2173*. [[CrossRef](#)]
35. Che, H.S.; Duran, M.; Levi, E.; Jones, M.; Hew, W.P.; Rahim, N.A. Post-fault operation of an asymmetrical six-phase induction machine with single and two isolated neutral points. In Proceedings of the 2013 IEEE Energy Conversion Congress and Exposition, Denver, CO, USA, 15–19 September 2013. [[CrossRef](#)]
36. Ghanooni, P.; Habibi, H.; Yazdani, A.; Wang, H.; Mahmoudzadeh, S.; Mahmoudi, A. Rapid Detection of Small Faults and Oscillations in Synchronous Generator Systems Using GMDH Neural Networks and High-Gain Observers. *Electronics* **2021**, *10*, 2637. [[CrossRef](#)]
37. Roshandel, E.; Mahmoudi, A.; Kahourzade, S.; Yazdani, A.; Shafiullah, G. Losses in Efficiency Maps of Electric Vehicles: An Overview. *Energies* **2021**, *14*, 7805. [[CrossRef](#)]

Disclaimer/Publisher’s Note: The statements, opinions and data contained in all publications are solely those of the individual author(s) and contributor(s) and not of MDPI and/or the editor(s). MDPI and/or the editor(s) disclaim responsibility for any injury to people or property resulting from any ideas, methods, instructions or products referred to in the content.